XLIII CILAMCE
21-25, November, 2022
FOZ DO IGUAÇU – PR – BRAZIL

Contact interaction law based on the Hertz theory for multibody applications

Lucas da Silva[1], Alfredo Gay Neto[1]

[1]*Dept. of Structural and Geotechnical Engineering, Polytechnic School at University of São Paulo*
Av. Prof. Luciano Gualberto, 380 - Butantã, 05508-010, São Paulo, Brazil
lucas7.silva@usp.br, alfredo.gay@usp.br

Abstract. The normal component of the contact interaction between two bodies arises from the fact that their material boundaries cannot go through each other. One way to deal with this non-penetration geometric constraint is to allow its violation on a controlled manner by adding an increasing magnitude force pair to the system, as long as the constraint violation increases. Methods that use this approach are usually referred as penalty-based methods. The simplest penalty method imposes a force proportional to the normal indentation. The proportionality constant acts as a stiffness parameter. An alternative interface law originates from Hertz's theory of nonconformal contact between elastic bodies. According to this classic theory, the contact force is proportional to the normal indentation raised to the power 3/2. The proportionality coefficient is not a constant, it has a dependency on the local curvatures of the contacting surfaces. Ultimately, the proportionality constant depends on the configuration of the system at a given time. In this work, we implement a penalty method based on Hertz force law for imposing contact between rigid bodies. The nonlinear dynamical equations for multibody dynamics are solved numerically. In the required linearization process, the dependency of the stiffness parameter on the degrees of freedom of the system is neglected. The results of the present method for a set of simple examples are presented. We verified that the considered simplification has a negative effect on the solution process if the stiffness varies throughout a time-step. The effect may be diminished using a large quantity of time-steps.

Keywords: Hertz contact theory, barrier method, multibody dynamics.

1 Introduction

Multibody dynamics involving contact interactions is of great importance for applications such as railway analysis [1]. In the treatment of the contact between rigid bodies by a penalty method, the constraint violation is measured by the normal indentation: the displacement along the normal direction to the contact plane required to separate the bodies. The indentation can be identified as a fictious penetration between rigid bodies, representing the actual local deformations on the surroundings of the contact patch, due to contact mechanical action. The simplest penalty method imposes a force proportional to the normal indentation. The proportionality constant acts as a stiffness parameter.

For applications requiring a more accurate relation between configuration of the system and contact forces, alternative interface laws based on constitutive relations may be employed. One such law originates from Hertz's theory of nonconformal contact between elastic bodies. According to this classic theory, the contact force is proportional to the normal indentation raised to the power 3/2. The proportionality coefficient is not a constant, it has a dependency on the local curvatures of the contacting surfaces. Ultimately, the proportionality constant depends on the configuration of the system at a given time.

In this work, we implement a penalty method based on Hertz force law for imposing contact between rigid bodies. The nonlinear equations for the contact interactions are solved numerically. In the required

linearization process, the dependency of the proportionality coefficient on the degrees of freedom of the system is neglected. The results of the present method for a set of examples are compared with some benchmarks. The objective is to verify if the considered simplification has a negative effect on the solution process.

2 Hertz contact theory

We present a quick summary of Hertz contact theory. A detailed exposition of this topic can be found in Johnson [2]. Hertz developed a solution for the problem of nonconformal contact of elastic bodies pressed against each other. The theory assumes that the contact patch formed around the initial contact point is elliptical. The basic parameter of the ellipse is its eccentricity $e = \sqrt{1 - k^2}$, where $k = b/a$, the ratio between the semi-minor axis b and the semi-major axis a, is called aspect ratio. Since $b \leq a$, k is in the range $(0, 1]$, implying e in the range $[0, 1)$. An ellipse with zero eccentricity is a circle of radius $r = a = b$, and the ellipse gets more elongated the more e approaches 1.

The surfaces of the bodies are supposed to be continuous up to the second derivative. Thus, it is possible to locally approximate them by quadratic polynomials in Cartesian coordinates of the tangent plane to the initial contact point. In the configuration of initial contact, the gap (or separation) between the surfaces measured in the orthogonal direction will also be represented by a quadratic polynomial. There is a suitable orientation of the coordinates in which the gap can be written as

$$h(x, y) = Ax^2 + By^2 \,, \tag{1}$$

where the coefficients A e B depend only on the principal curvatures and principal directions of the surfaces.

By pressing the bodies against each other with a given load, points distant from the contact region translate as rigid. The approach of the bodies due to the rigid displacements is called indentation and is denoted by δ. A semi-ellipsoidal pressure distribution over the contact patch produces the elastic displacements that balance the rigid displacements in accordance with the fundamental geometric condition of contact, i.e., after the deformation, points in the contact patch have no separation and points not in the contact patch remain separated.

A relation between the quadratic approximation coefficients and the eccentricity of the contact ellipse is given by

$$\frac{B}{A} = \frac{E(e)/\left(1-e^2\right)-K(e)}{K(e)-E(e)} \,, \tag{2}$$

where K and E are the complete elliptic integrals of first and second kind respectively. This nonlinear equation can be solved numerically for e.

The values of A and B depend only on the local geometry of the surfaces, and so does the eccentricity of the contact ellipse. The load is responsible for the size of the ellipse. The following proportionality rule holds

$$c \equiv (ab)^{1/2} \propto P^{1/3} \,. \tag{3}$$

Another result of Hertz theory is a relation between the load P and the indentation δ in the form of a force law

$$P = \varepsilon \, \delta^{3/2} \tag{4}$$

with a stiffness parameter

$$\varepsilon = \frac{4E^*}{3} \left\{ \frac{R_e}{[F_2(e)]^3} \right\}^{1/2} \tag{5}$$

where E^* is a reduced elastic parameter dependent on the elastic properties (Young's modulus and Poisson's ratio) of both bodies and R_e is an equivalent radius of curvature obtained by combining the principal radii of both surfaces.

3 Contacting surfaces

As we have seen in the previous section, the curvatures of the contact surfaces determine the eccentricity of the contact ellipse and the contact stiffness. Extrusion and revolution surfaces are herein considered for their principal curvatures and principal directions are easy to compute in any point, besides their practical applications.

3.1 Revolution surfaces

A surface of revolution is the set of points swiped by a generator curve rotated about a given axis. If the generator is a plane curve and the axis of rotation is in the same plane, then every plane containing the axis intersects the surface in two copies of the generator, which are called meridians. The curvature of the meridian through a point is a principal curvature of the surface at the point because the plane of the meridian is a plane of symmetry of the surface. The principal direction associated with this curvature is the tangent vector to the meridian.

The second principal direction is orthogonal to the first, it is the tangent vector to the circle in the intersection of the surface and the plane orthogonal to the axis passing through the point. The radius of this circle, denoted by ρ, equals the distance from the point to the axis. The principal curvature is

$$k_2 = \frac{\cos\alpha}{\rho} \tag{6}$$

where α is the angle between the normal to the axis and the normal of the generator curve (see Figure 1).

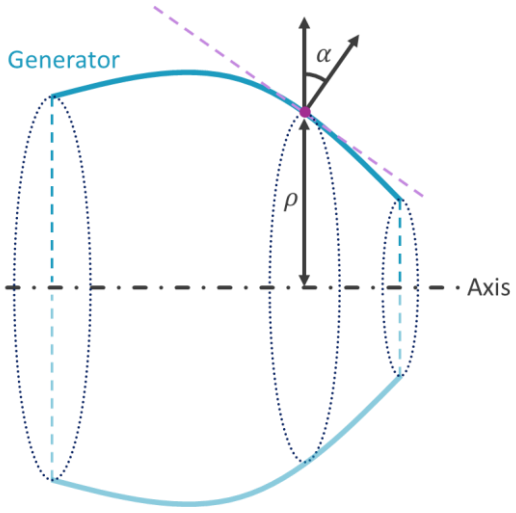

Figure 1 – Radial section of a revolution surface

3.2 Extrusion surfaces

A surface of extrusion is the set of points swiped by a generator curve translated along a given straight line. If a plane contains the generator curve and the extrusion occurs in the orthogonal direction, then the intersections of parallel planes and the surface are copies of the generator. The curvature of a copy of the generator through a point coincides with the first principal curvature at the point.

The vector parallel to the line of extrusion is the other principal direction. The associated principal curvature is zero.

Remark 1: Sign of the curvatures. Johnson adopts the convention in which a non-zero curvature is positive when measured along a convex direction of the surface and negative otherwise. The same convention was adopted in present work, as Equation (2) is based on it.

Remark 2: Arc-based surfaces. If the generator curve is part of a circle, then its curvature is a constant equal to

the inverse of the radius. In the conditions discussed previously, this constant curvature is a principal curvature in any point of both types of surfaces.

4 Hybrid barrier method

The calculations were integrated into a generic framework for finite elements and multibody dynamics (GIRAFFE [3]) developed by Prof. Alfredo at University of São Paulo. The framework also deals with computational contact mechanics. A particular implementation of contact mechanics available follows a surface-to-surface pointwise contact approach. The approach was first introduced in Gay Neto, Pimenta, and Wriggers [4] for the contact of beam elements in a Finite Elements context. It was later expanded to allow the interaction with rigid body elements in Campos and Gay Neto [5].

Gay Neto and Wriggers [6] present a formulation for contact enforcement. The formulation combines a barrier-type force, inversely proportional to a power of the (normal) gap g_n between the contact points, and a physically sensible force law

$$f_n(g_n) = \begin{cases} 0 & \text{if } g_n \geq \bar{g}_n \\ \epsilon_1(\bar{g}_n - g_n)^{n_1} & \text{if } \bar{\bar{g}}_n \leq g_n < \bar{g}_n \\ \epsilon_2 g_n^{n_2} + c_2 & \text{if } g_n < \bar{\bar{g}}_n \end{cases}. \tag{7}$$

As seen in Equation (7) the behaviors are separated by thresholds. The first threshold $\bar{g}_n$ controls the activation of the contact reaction, if g_n is greater than $\bar{g}_n$, then there is no force. The second threshold $\bar{\bar{g}}_n$ controls the activation of the barrier. The barrier is used to prevent penetrations of the contact surfaces making contact detection easier. The thresholds are user-defined. The parameters ϵ_2 and c_2 are not independent, they are set such that the function f_n is continuous to the first derivative at $\bar{\bar{g}}_n$.

The term $\bar{g}_n - g_n$ in parentheses can be identified with an indentation δ as it measures how much the surfaces have approached since they were close enough to activate contact. So the force is proportional to a power of the indentation exactly as the Hertzian force law in Equation (4). Setting the power to $n_1 = 3/2$ and ϵ_1 to the stiffness parameter given by Equation (5) configures a model of the Hertzian contact.

When used to enforce the contact between rigid bodies, this model can reproduce the part of the static behavior of elastic bodies regarding the load-indentation relation.

5 Numerical examples

In this section, two basic examples are presented to verify the behavior of the contact model. For all bodies, we consider the same material with elastic parameters $E = 2$ GPa and $\nu = 0.3$, hence the reduced elastic parameter of a contact pair is $E^* = 1.0989$ GPa.

The examples consist of the motion of a rigid body element (a node with 3 translational and 3 rotational degrees of freedom) attached to a rigid contact surface against another rigid contact surface. The nonlinearity of the force law results in nonlinear equations of motion that are solved using Newton-Raphson method.

5.1 Contact of a sphere and a plane

In this example, a sphere of unit radius is pressed against a flat plane (Figure 2). These surfaces have the special property that the curvature is the same in any point along any direction, which means that the principal curvatures are equal. For the sphere, the principal curvatures equal the inverse of the radius, which is 1 m in this case. For the plane, the principal curvatures are zero. This geometry results in $A = B = 0.5$ [m^{-1}], the eccentricity of the contact patch is $e = 0$ (a circle), and the equivalent radius is $R_e = 1$ m (equal to the sphere's radius). The stiffness parameter has numerical value $\varepsilon = 1.4652 \times 10^9$ in SI units.

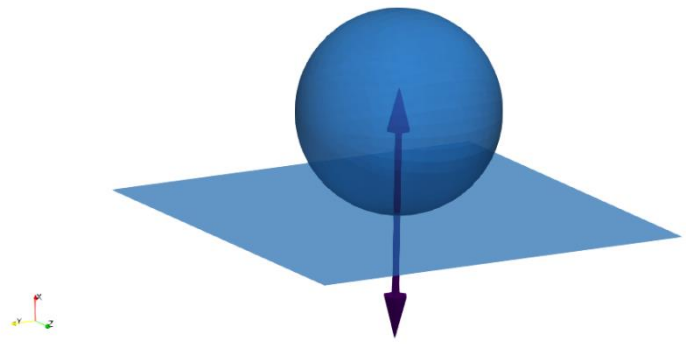

Figure 2 – Contact of a sphere and a plane

The node of the rigid body element is attached to the center of the sphere. A displacement of 1 cm perpendicular to the plane is progressively (10 static time-steps) applied to this node. The remaining degrees of freedom are fixed. Figure 3 shows the contact force that reacts to this indentation. The force obtained using GIRAFFE is labeled "numerical". It is compared with the force predicted by Equation (4) using the same ε, labeled "analytical".

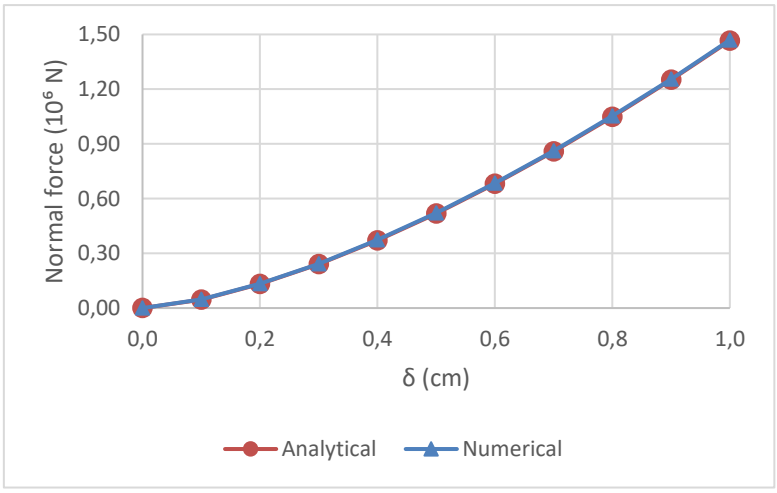

Figure 3 – Force versus indentation

The two plots are in good agreement. The value of the maximum force is 1.4696×10^6 N for the numerical solution while the correct value is 1.4652×10^6 N.

5.2 Two cylinders

Two cylinders of unit radius with axes parallel to the horizontal plane and orthogonal to each other are put into contact (Figure 4). Then, the top cylinder is slowly (static time-steps) rotated about the vertical axis at a constant rate. As the aspect ratio of the contact ellipse depends on the angle between the axes, the contact stiffness changes with the imposed rotation. The contact force must also vary to keep constant the distance between the cylinders.

The principal curvatures of the surfaces are 1 $[\mathrm{m}^{-1}]$, the inverse of the radius, and zero. In the initial configuration, the geometry of the contact ellipse is the same as in the previous example. As the rotation progresses, the contact ellipse becomes slenderer, and the contact stiffness increases. At the end of each time-step, the stiffness parameter is updated for the current configuration and kept constant until the next.

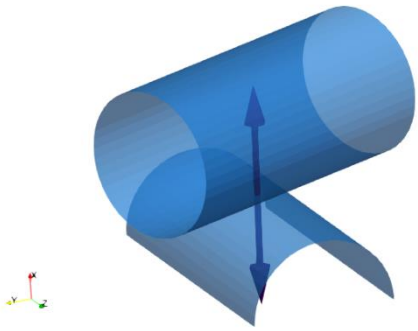

Figure 4 – Contact of two cylinders

Two simulations were performed, one with ten time-steps and other with 100 time-steps. The relationship between force and angle is shown in Figure 5. In the initial configuration (perpendicular cylinders), the force coincides with the maximum force of the previous example since the stiffness is the same and the indentation is set to be 1 cm. The force, then, increases as the cylinders approach alignment.

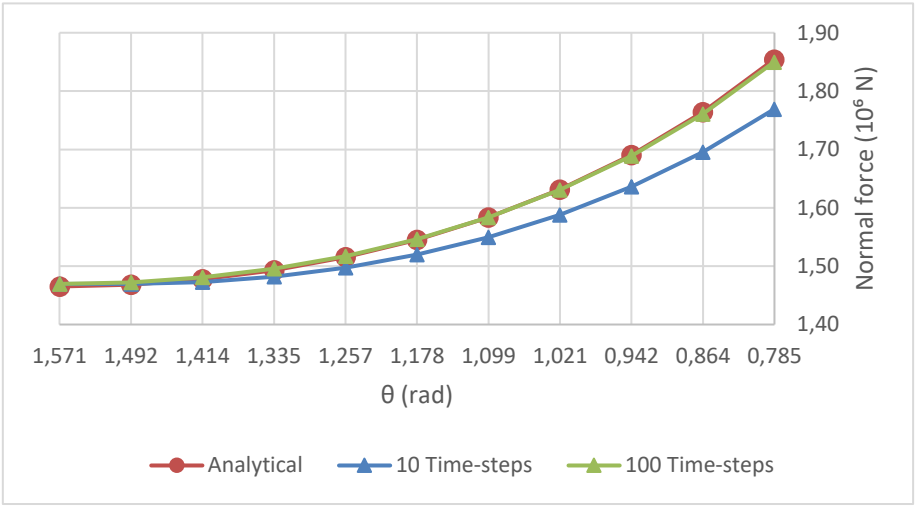

Figure 5 – Force versus angle for a constant indentation of 1 cm

In Figure 5, we can see that the numerical solution diverges from the analytical solution when the number of time-steps is small. This occurs because the stiffness parameter has a constant value throughout a time-step despite its dependency on a varying coordinate of the system, the angle θ.

The apparent divergence is a delay in the computation of the force. Since the value of the stiffness parameter is computed at the start of a time-step, the obtained force at the end balances the previous configuration and not the current one. In this static setting, in which the configurations are prescribed, the results can be easily corrected by shifting the forces to the correct configurations. In a dynamic setting, however, the configurations are not known beforehand. A possible correction is to update the stiffness parameter along with the degrees of freedom throughout the time-step.

6 Conclusions

We successfully implemented a particularization of the general interface law presented in [6] that models the behavior of Hertzian contact. The basic examples presented show that in static settings the relationship between indentation and contact force obtained by GIRAFFE's numerical framework agrees with the contact theory. The number of time-steps must be large enough to guarantee the convergence of the contact force to the theoretical value in cases where the stiffness parameter is not constant. The divergence observed otherwise may also be corrected by updating the stiffness parameter at each iteration of the method used to compute the solution of the nonlinear equations of motion. The convergence of the Newton-Raphson method here used was not impaired in the example tested.

Acknowledgements. The authors acknowledge Vale S.A. for the financial support under the wheel-rail contact chair. The second author acknowledges CNPq (Conselho Nacional de Desenvolvimento Científico e Tecnológico) under the grant 304321/2021-4.

Authorship statement. The authors hereby confirm that they are the sole liable persons responsible for the authorship of this work, and that all material that has been herein included as part of the present paper is either the property (and authorship) of the authors, or has the permission of the owners to be included here.

References

[1] A. A. Shabana, M. Tobaa, H. Sugiyama and K. E. Zaazaa. "On the Computer Formulations of the Wheel/Rail Contact Problem," Nonlinear Dynamics, vol. 40, n. 2, pp. 169-193, 2005.
[2] K. L. Johnson. *Contact mechanics.* Cambridge University Press, 1985.
[3] A. Gay Neto, "Giraffe User's Manual - Generic Interface Readily Accessible for Finite Elements," 2021. [Online]. Available: http://sites.poli.usp.br/p/alfredo.gay/.
[4] A. Gay Neto, P. M. Pimenta and P. Wriggers, "A master-surface to master-surface formulation for beam to beam contact. Part I: frictionless interaction," Computer Methods in Applied Mechanics and Engineering, vol. 303, pp. 400-429, 2016.
[5] P. R. Refachinho de Campos e A. Gay Neto, "Rigid body formulation in a finite element context with contact interaction," Computational Mechanics, vol. 62, n. 6, pp. 1369-1398, 2018.
[6] A. Gay Neto and P. Wriggers, "Discrete element model for general polyhedra," Computational Particle Mechanics, vol. 9, n. 2, pp. 353-380, 2021.